

Mutant *LRRK2*^{R1441G} BAC transgenic mice recapitulate cardinal features of Parkinson's disease

Yanping Li^{1,5}, Wencheng Liu^{1,5}, Tinmarla F Oo², Lei Wang^{1,3}, Yi Tang^{1,4}, Vernice Jackson-Lewis², Chun Zhou², Kindiya Geghman¹, Mikhail Bogdanov^{1,3}, Serge Przedborski², M Flint Beal¹, Robert E Burke² & Chenjian Li¹

Mutations in leucine-rich repeat kinase 2 (*LRRK2*) are the most common genetic cause of Parkinson's disease. We created a *LRRK2* transgenic mouse model that recapitulates cardinal features of the disease: an age-dependent and levodopa-responsive slowness of movement associated with diminished dopamine release and axonal pathology of nigrostriatal dopaminergic projection. These mice provide a valid model of Parkinson's disease and are a resource for the investigation of pathogenesis and therapeutics.

LRRK2 is the causative gene for PARK8 type Parkinson's disease with autosomal dominant inheritance^{1,2}. Mutations in *LRRK2* are the most common genetic cause of familial and nonfamilial Parkinson's disease^{3–5}. Most individuals with *LRRK2* mutations have dopamine neuron loss in substantia nigra and Lewy body pathology, typical features of idiopathic Parkinson's disease⁶. Notably, some individuals with *LRRK2* mutations also have tauopathy in the absence of Lewy

pathology. Tauopathy and hyperphosphorylated tau are common features of several neurodegenerative diseases^{7,8}. The pathogenesis of Parkinson's disease resulting from *LRRK2* mutations and the more common sporadic forms remains elusive, and a major obstacle to research has been the lack of valid mouse models that recapitulate some of hallmarks of the Parkinson's disease phenotype⁹.

To generate *LRRK2* transgenic mouse models, we obtained a human bacterial artificial chromosome (BAC) clone containing full length *LRRK2* and verified it by sequencing (**Supplementary Methods** online). The BAC clone was engineered and confirmed to carry R1441G, a common missense mutation in large family pedigrees and with nearly complete penetrance^{1,2} (**Supplementary Figs. 1–3** online).

Both wild-type and *LRRK2*^{R1441G} transgenic mice were generated (**Supplementary Fig. 4** online). Among independent transgenic mouse lines, the RP135 and RP57 lines expressed *LRRK2*^{R1441G} approximately five- to tenfold above the level of endogenous mouse *Lrrk2* (**Supplementary Fig. 5** online). Transgene expression was detected in the cortex, cerebellum, striatum and ventral midbrain (**Supplementary Fig. 5**), consistent with previous reports¹⁰. The *LRRK2*^{R1441G} mice developed normally. At 3 months of age, there was no deficit in body weight, brain weight (data not shown) or motor activity (**Fig. 1a**).

The *LRRK2*^{R1441G} mice, but not nontransgenic littermate controls, had age-dependent and progressive motor-activity deficits, beginning with reduced mobility that was reminiscent of hypokinesia in Parkinson's disease. By 10–12 months of age, the hypokinesia in most *LRRK2*^{R1441G} mice had progressed to a visually apparent immobility, reminiscent of akinesia in late Parkinson's disease, in the absence of weakness. These motor deficits in 10–12-month-old *LRRK2*^{R1441G} mice were observed in both home cage activity (**Supplementary Video 1** online) and open field (**Supplementary Videos 2 and 3** online), and

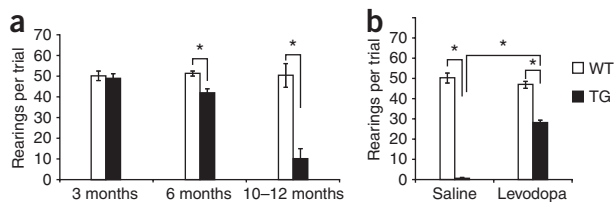


Figure 1 *LRRK2*^{R1441G} BAC mice develop age-dependent motor deficits that responds to levodopa and apomorphine. (a) An age-dependent decline in rearing was detected from 3 to 6 months (wild-type nontransgenic littermates (WT), $n = 5$; *LRRK2*^{R1441G} BAC mice (TG) $n = 5$; $P = 0.005$). At 10–12 months, *LRRK2*^{R1441G} BAC mice had more significant reductions in rearing (WT, $n = 14$; TG, $n = 17$; $P = 0.001$). (b) This robust deficit in *LRRK2*^{R1441G} BAC mice was rescued by 20 mg per kg of body weight of levodopa with 6.25 mg per kg of benserazide but not by 2 mg per kg of levodopa. A similar rescue was achieved by 10 mg per kg of apomorphine. Data are presented as mean \pm s.e.m. Asterisks indicate statistically significant differences ($P < 0.05$).

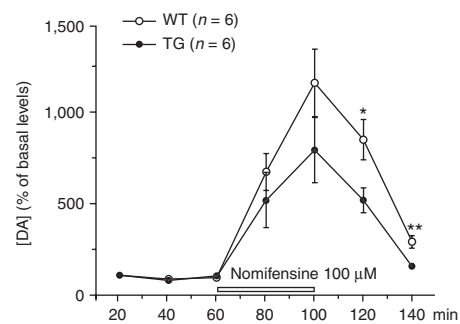


Figure 2 Neurochemical deficits in *LRRK2*^{R1441G} mice. In the presence of nomifensine, striatal dopamine release was significantly decreased in freely moving *LRRK2*^{R1441G} BAC mice, as seen by microdialysate analysis ($F_{1,16} = 5.7$, $P = 0.03$, two-way ANOVA). Total spontaneous dopamine release, calculated as the area under the curve above baseline, was significantly decreased (35%, $P = 0.03$, two way ANOVA and Mann-Whitney test). [DA], dopamine concentration.

¹Department of Neurology and Neurosciences, Weill Medical College of Cornell University, New York, New York, USA. ²Departments of Neurology and Pathology, Columbia University, New York, New York, USA. ³Bedford Veterans Administration Medical Center, Bedford, Massachusetts, USA. ⁴Present address: Department of Neurology, Xuan-Wu Hospital, Beijing, China. ⁵These authors contributed equally to this work. Correspondence should be addressed to C.L. (chl2011@med.cornell.edu).

were confirmed and quantified by the cylinder test (**Fig. 1a** and **Supplementary Videos 4** and **5** online). Levodopa and a direct-acting dopamine agonist, apomorphine, both reversed the deficits in the above-mentioned tasks in mice with severe motor deficits (**Fig. 1b** and **Supplementary Videos 6–8** online). Thus, the *LRRK2^{R1441G}* transgenic mice faithfully recapitulated the progressive motor deficits and responsiveness to levodopa that are characteristic of human Parkinson's disease.

We also generated transgenic mice that overexpressed wild-type *LRRK2* (WT-OX). The transgene expression in WT-OX mice was comparable to that in *LRRK2^{R1441G}* mice (**Supplementary Fig. 6** online). The WT-OX mice developed normally and did not demonstrate progressive motor behavioral deficits (**Supplementary Fig. 6**). Therefore, the phenotypes that we observed in *LRRK2^{R1441G}* mice were the results of the mutation rather than an overexpression of the *LRRK2* protein.

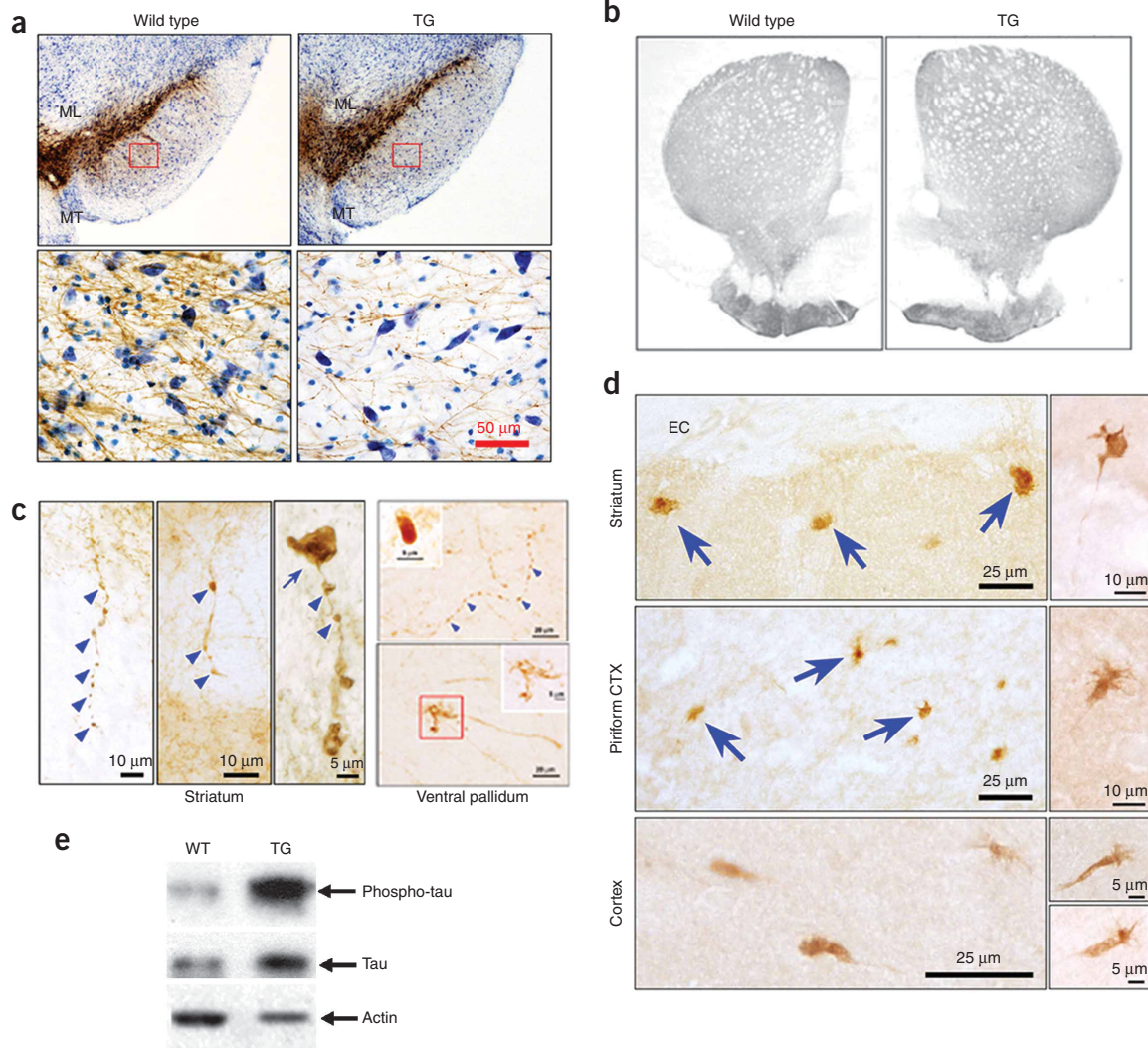


Figure 3 Morphologic abnormalities of mesencephalic dopamine neurons and their axons in *LRRK2^{R1441G}* BAC transgenic mice. **(a)** Tyrosine hydroxylase immunostaining of ventral mesencephalon. ML, medial lemniscus; MT, medial terminal nucleus. Rectangles in the upper panels are shown at a higher magnification in the lower panels. *LRRK2^{R1441G}* BAC transgenic mice showed a loss of tyrosine hydroxylase-positive dendrites in substantia nigra pars reticulata and a reduction of tyrosine hydroxylase neuron size in SNpc. **(b)** Normal optical density of tyrosine hydroxylase immunostaining of the whole striatum and dorsal-lateral quadrant. **(c)** In tyrosine hydroxylase-positive axons in the striatum and the ventral pallidum of *LRRK2^{R1441G}* BAC transgenic mice, we observed discrete foci of thickening with a beaded appearance (blue arrowheads) and fragmentation, large tyrosine hydroxylase-positive spheroid-like structures (blue arrow in the left panel and the insert in the upper right panel), and dystrophic neurites and enlarged axonal endings (lower right). The dystrophic neurites were found in all of the five *LRRK2^{R1441G}* mice (2.8 ± 0.6 , s.e.m.) but were rarely seen in two of the seven nontransgenic littermates (0.4 ± 0.3 ; $P = 0.003$, t test). Dystrophic neurites were not found in the two WT-OX mice. Thus, expressed as number of neurites per area of the ventral pallidum (mm^2), dystrophic neurites were 8.5-fold more prevalent among the transgenic mice than the controls. **(d)** In the dorsal striatum and piriform cortex, immunohistochemistry with AT8 revealed abnormal axon terminal enlargements and dystrophic neurites (arrows, top two left panels). EC, external capsule. AT8-positive structures are shown at a higher magnification in the right panels. A total of 42 AT8-positive dystrophic neurites were identified in the two *LRRK2^{R1441G}* mice that we examined. A single example was identified under blind conditions in one of the four nontransgenic mice, and none were found in the two WT-OX mice. Expressed as the number of neurites per forebrain coronal hemisection, 21 AT8-positive neurites were observed among the *LRRK2^{R1441G}* transgenics and only 0.17 among the control brains, a 124-fold difference. **(e)** Phosphorylated tau was markedly increased in the *LRRK2^{R1441G}* BAC transgenic mouse brains. Full-size western blots are presented in **Supplementary Figure 7** online.

To explore whether the hypokinesia in *LRRK2^{R1441G}* mice was associated with a deficiency of striatal dopamine as in human Parkinson's disease, we carried out intrastriatal microdialysis in awake and freely moving mice. In the presence of the dopamine re-uptake blocker nomifensine, we observed a significant reduction of extracellular dopamine in *LRRK2^{R1441G}* mice ($P = 0.03$; **Fig. 2**), indicating that dopamine release was indeed impaired.

In histological analysis, there was no observable cell death or gliosis in the spinal cord, and we found no general abnormalities in brain structures in 9–10-month-old *LRRK2^{R1441G}* transgenic mice (data not shown). Immunohistochemistry for tyrosine hydroxylase in 9–10-month-old *LRRK2^{R1441G}* mice revealed that dopaminergic neurons in the substantia nigra pars compacta (SNpc) (A9) and ventral tegmental area (A10) were normal in number and anatomical organization (**Fig. 3a** and **Supplementary Methods**). We identified two abnormalities of the SNpc dopamine neurons: a decrease (8%, $P = 0.01$) in average cell body size and a marked diminution in the number of tyrosine hydroxylase-positive dendrites (29%, $P = 0.007$) in the substantia nigra pars reticulata (**Fig. 3a** and **Supplementary Methods**).

Although the overall pattern and optical density of tyrosine hydroxylase immunostaining in the striatum of *LRRK2^{R1441G}* mice appeared normal (**Fig. 3b** and **Supplementary Methods**), profound abnormalities were observed at the cellular level in *LRRK2^{R1441G}* mice, but not in nontransgenic littermate controls or WT-OX mice. In *LRRK2^{R1441G}* mouse striatum and piriform cortex, two areas that were enriched in dopaminergic projections, tyrosine hydroxylase-positive axons appeared to be beaded and fragmented and exhibited spheroids and dystrophic neurites (**Fig. 3c,d** and **Supplementary Methods**), as described in other forms of axonal injury^{11–13}. Axonal pathology of fragmentation and spheroid formation has been observed in the striata of individuals with Parkinson's disease¹⁴.

Given that tauopathy has been identified in the brains of individuals with Parkinson's disease resulting from *LRRK2* mutations, we performed immunohistochemistry with the AT8 monoclonal antibody, which recognizes a phosphorylated tau epitope¹⁵. In dorsal striatum and piriform cortex of *LRRK2^{R1441G}* mice, but not in nontransgenic littermate control or WT-OX mice, we observed AT8 immunopositive

abnormal axonal swellings and dystrophic neurites, similar to those defined by tyrosine hydroxylase staining (**Fig. 3d**). Furthermore, biochemical analysis revealed that tau is hyperphosphorylated in brain tissues of *LRRK2^{R1441G}* transgenic mice (**Fig. 3e**).

LRRK2^{R1441G} BAC transgenic mice offer, for the first time, a model of Parkinson's disease, derived from a known genetic cause, that successfully recapitulates the motor behavioral, neurochemical and histopathological features of the human disease. These mice will be a powerful tool for *in vivo* mechanistic studies and therapeutic development.

Note: Supplementary information is available on the Nature Neuroscience website.

ACKNOWLEDGMENTS

We wish to thank K. Merchant and her team at Eli Lilly and Company for generating the immunoblot data that facilitated selection of transgenic lines, S. Fleming and M.-F. Chesselet for advice on behavioral studies, and X. William Yang and A. Yamamoto for insightful discussions. This work was supported in part by grants from the Michael J. Fox Foundation and the US National Institutes of Health to C.L., from the Department of Defense to M.F.B., and from US National Institutes of Health and the Parkinson's Disease Foundation to R.E.B. and T.F.O.

Published online at <http://www.nature.com/natureneuroscience/>
Reprints and permissions information is available online at <http://www.nature.com/reprintsandpermissions/>

1. Zimprich, A. *et al. Neuron* **44**, 601–607 (2004).
2. Paisán-Ruiz, C. *et al. Neuron* **44**, 595–600 (2004).
3. Di Fonzo, A. *et al. Lancet* **365**, 412–415 (2005).
4. Gilks, W.P. *et al. Lancet* **365**, 415–416 (2005).
5. Saunders-Pullman, R. *et al. Neurosci. Lett.* **402**, 92–96 (2006).
6. Polymeropoulos, M.H. *et al. Science* **276**, 2045–2047 (1997).
7. Ballatore, C., Lee, V.M. & Trojanowski, J.Q. *Nat. Rev. Neurosci.* **8**, 663–672 (2007).
8. Tobin, J.E. *et al. Neurology* **71**, 28–34 (2008).
9. Dauer, W. & Przedborski, S. *Neuron* **39**, 889–909 (2003).
10. Melrose, H.L. *et al. Neuroscience* **147**, 1047–1058 (2007).
11. El-Khodor, B.F. & Burke, R.E. *J. Comp. Neurol.* **452**, 65–79 (2002).
12. Büki, A., Okonkwo, D.O., Wang, K.K. & Powlislock, J.T. *J. Neurosci.* **20**, 2825–2834 (2000).
13. Kerschensteiner, M., Schwab, M.E., Lichtman, J.W. & Misgeld, T. *Nat. Med.* **11**, 572–577 (2005).
14. Duda, J.E., Giasson, B.I., Mabon, M.E., Lee, V.M. & Trojanowski, J.Q. *Ann. Neurol.* **52**, 205–210 (2002).
15. Biernat, J. *et al. EMBO J.* **11**, 1593–1597 (1992).